The long Filamin-A isoform is required for intestinal development and motility: implications for chronic intestinal pseudo-obstruction

Zada, A.; Zhao, Y.Y.; Halim, D.; Windster, J.; Linde, H.C. van der; Glodener, J.; ... ; Alves, M.M.

OXFORD

Human Molecular Genetics, 2023, Vol. 32, 1, 151–160
https://doi.org/10.1093/hmg/ddac199
Advance access publication date 18 August 2022
Original Article

The long Filamin-A isoform is required for intestinal development and motility: implications for chronic intestinal pseudo-obstruction

Almira Zada[1,†], Yuying Zhao[1,2,†], Danny Halim[1], Jonathan Windster[1,3], Herma C. van der Linde[1], Jackleen Glodener[4], Sander Overkleeft[1], Bianca M. de Graaf[1], Robert M. Verdijk[5], Alice S. Brooks[1], Iain Shepherd[4], Ya Gao[2], Alan J. Burns[1,6,‡], Robert M.W. Hofstra[1,6] and Maria M. Alves[1,*]

[1]Department of Clinical Genetics, Erasmus University Medical Center, Sophia Children's Hospital, Rotterdam 3015GD, The Netherlands
[2]Department of Pediatric Surgery, The Second Affiliated Hospital of Xi'an Jiaotong University, Xi'an, Shaanxi 710004, China
[3]Department of Pediatric Surgery, Erasmus University Medical Center Rotterdam, Sophia Children's Hospital, Rotterdam 3015GD, The Netherlands
[4]Department of Biology, Rollins Research Center, Emory University, Atlanta, GA 30322, USA
[5]Department of Pathology, Erasmus University Medical Center, Rotterdam 3015GD, The Netherlands
[6]Birth Defects Research Centre, UCL Great Ormond Street Institute of Child Health, London WC1N 1EH, UK
*To whom correspondence should be addressed at: Department of Clinical Genetics, Erasmus University Medical Center, Sophia Children's Hospital, PO Box 2040, 3000CA Rotterdam, The Netherlands. Tel: +3110-7030683; Email: m.alves@erasmusmc.nl
†Equal contribution.
‡Present address: Gastrointestinal Drug Discovery Unit, Takeda Developmental Center Americas, Inc, Cambridge, USA.

Abstract

Filamin A (FLNA) is a cytoplasmic actin binding protein, recently shown to be expressed as a long and short isoform. Mutations in *FLNA* are associated with a wide spectrum of disorders, including an X-linked form of chronic intestinal pseudo-obstruction (CIPO). However, the role of FLNA in intestinal development and function is largely unknown. In this study, we show that FLNA is expressed in the muscle layer of the small intestine from early human fetal stages. Expression of *FLNA* variants associated with CIPO, blocked expression of the long flna isoform and led to an overall reduction of RNA and protein levels. As a consequence, contractility of human intestinal smooth muscle cells was affected. Lastly, our transgenic zebrafish line showed that the *flna* long isoform is required for intestinal elongation and peristalsis. Histological analysis revealed structural and architectural changes in the intestinal smooth muscle of homozygous fish, likely triggered by the abnormal expression of intestinal smooth muscle markers. No defect in the localization or numbers of enteric neurons was observed. Taken together, our study demonstrates that the long FLNA isoform contributes to intestinal development and function. Since loss of the long FLNA isoform does not seem to affect the enteric nervous system, it likely results in a myopathic form of CIPO, bringing new insights to disease pathogenesis.

Introduction

Filamin A (FLNA) is a cytoplasmic protein with a well-characterized role. It was the first actin filament cross linking protein to be identified in non-muscle cells, and is involved in a series of events required for cell motility, migration and maintenance of cytoskeletal integrity (1,2). Several binding partners are known for FLNA, including ion channels, receptors, intracellular signalling molecules and transcription factors (2). Therefore, it is not surprising that loss of function variants affecting the normal expression levels of FLNA are associated with various human disorders (3–8). These disorders are frequently called filaminopathies, and show a wide phenotypic variability, including abnormal neuronal migration, as well as vascular and cardiac defects, and intestinal dysmotility characteristic of chronic intestinal pseudo-obstruction (CIPO) (4).

CIPO encompasses a heterogeneous group of disorders of which, Congenital Short Bowel Syndrome (CSBS), Megacystis Microcolon Intestinal Hypoperistaltic Syndrome (MMIHS) and Hirschsprung disease (HSCR) are examples of severe forms. Several genes have been identified as the cause of neuronal and myopathic forms of CIPO, and depending on the affected gene, various degrees of intestinal dysmotility have been reported (9,10). *FLNA* is one of the genes previously described to cause an X-linked form of CIPO. Two independent studies reported the presence of two base pair (bp) deletions in this gene (NM_001110556.2: c.16-17delTC, c.65-66 del AC) in five male patients diagnosed with CIPO associated CSBS (8,11). These deletions, located in exon two of *FLNA*, result in a frameshift with the subsequent appearance of an early stop codon a few bps later. Interestingly, exon two of *FLNA* has a peculiarity, the presence of two methionine's separated by 28 amino acids. Due to this feature, it has been suggested that two FLNA isoforms exist, and that in the presence of the two bp deletions, only expression of the long isoform is affected (11). This hypothesis was recently confirmed by the identification of three distinct transcription start sites in *FLNA*, while studying the pathogenicity of another *FLNA* deletion (NM_001110556.2: c.18-19delTC) identified in a CIPO patient (12). Two of these sites were shown to produce a protein isoform using the first methionine

Received: March 1, 2022. **Revised:** August 2, 2022. **Accepted:** August 9, 2022

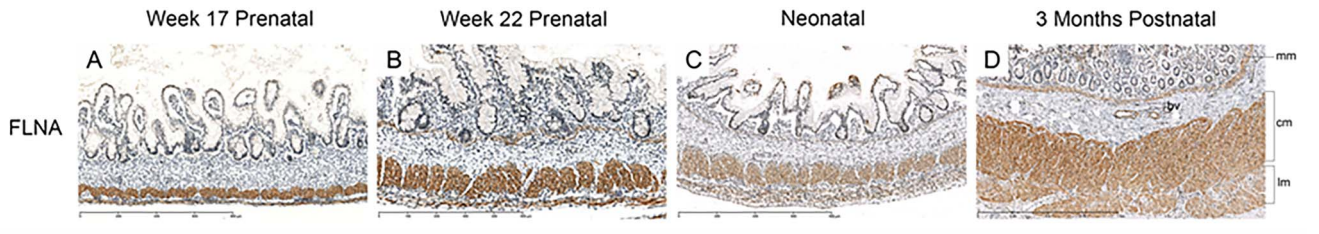

Figure 1. FLNA expression is present in the muscular layer of the human small intestine from early fetal stages. FLNA immunohistochemistry (brown stain) performed in human intestinal specimens collected at different developmental stages shows that FLNA is expressed in the muscular layer of the small intestine. mm: muscularis mucosa; cm: circular layer of the muscularis propria; lm: longitudinal layer of the muscularis propria.

(ATG^{+1}), while the third one used a methionine located 81 nucleotides after the first starting site (ATG^{+82}). Moreover, tissue-specific regulation of FLNA was reported during development, with the long FLNA isoform being predominantly expressed in intestinal smooth muscle, while the short isoform was more abundant in other tissues/organs, including the brain (12). Despite these findings, the role of FLNA in intestinal development is still poorly understood, making it difficult to pinpoint the pathogenic mechanisms involved in the development of CIPO.

In this study, we bring new insights into the role of FLNA, by further investigating the existence of two FLNA isoforms, and providing evidence that the long isoform is required for smooth muscle contractility, intestinal elongation and intestinal motility.

Results

FLNA is expressed in the muscle layers of the human small intestine

FLNA is a cytoplasmic protein that is ubiquitously expressed in all tissues of the body. However, not much is known about FLNA expression during human development. Since CIPO is characterized by intestinal dysmotility, we investigated the expression of FLNA in the human intestine (jejunum/ileum) at weeks 17 and 22 of fetal development, at the neonatal stage and postnatally (3-months old). At all developmental stages, FLNA was abundantly expressed in the cytoplasm of smooth muscle cells, including smooth muscle cells of the muscularis mucosa (mm), and the inner circular layer (cm) and outer longitudinal layer (lm) of the muscularis propria (Fig. 1).

Expression of the long FLNA isoform is disrupted in CIPO patients

Recently, it has been shown that a deletion of two bps in *FLNA* (c.18-19delTC) in a CIPO patient, led to disruption of the long FLNA isoform (12). Since the two bp deletions found in other CIPO patients (c.16-17delTC, c.65-66delAC), are also located between the two methionine residues shown to be distinct transcription sites (Fig. 2A), we hypothesized a similar outcome for these deletions, i.e. disruption of the long FLNA isoform. To investigate that indeed an alternative initiation codon was used in the presence of the two bp deletions, we used a mini-gene construct previously described (11), where only exon two of *FLNA* (WT) is present, fused to an HA-tag. By expressing constructs containing the WT, c.16-17delTC (Mut1) and c.65-66delAC (Mut2), in HEK293 cells we observed that FLNA WT produced 2 bands, showing the existence of two initiation codons in FLNA (Fig. 2B). However, in the presence of any of the deletions, Mut1 or Mut2, only the lower band was detected (Fig. 2B), showing that in these cases only the second initiation codon is active.

To further study the impact of the two bp deletions in the total expression levels of FLNA, we overexpressed a construct containing FLNA WT, Mut1 and Mut2, tagged C-terminally with a Myc-tag, in HEK293 cells. We subsequently determined the levels of *FLNA* messenger RNA (mRNA) and protein, by quantitative real time (qRT)-PCR and western blot (WB), respectively. Our results showed that the presence of the two bp deletions lead to reduced levels of FLNA, both at mRNA and protein levels (Fig. 2C and D).

The long FLNA isoform is required for contractility of intestinal smooth muscle cells

Our immunohistochemistry studies showed that FLNA is expressed in the smooth muscle of the intestine at different human developmental stages. Since the smooth muscle plays an important role in intestinal peristalsis, we decided to evaluate whether the 2 bp deletions in *FLNA* affect contraction of human intestinal smooth muscle cells (hISMCs). For this purpose, we transfected hIMSCs with constructs expressing the WT FLNA protein and the two 2 bp deletions associated with CIPO, Mut1 (c.16-17delTC) and Mut2 (c.65-66delAC). Untransfected cells (Un) were used as control. We then performed *in vitro* contractility assays, based on the contraction of a collagen matrix. Cellular contractility was calculated by measuring the total area occupied by the collagen matrix at time 0 (Initial Area (Ai)) and 24 hours after detachment (Final area (Af)) of the matrix from the wells. Our results showed that overexpression of FLNA leads to an increase in cellular contractility, whereas expression of Mut1 and Mut2 showed no significant effect when compared with the control (Fig. 3A and B). This result is likely due to the lower amounts of FLNA produced when the two deletions (Mut1 and Mut2) are present, showing that FLNA levels are instrumental for intestinal smooth muscle contractility.

Generation of the *flna* long isoform knockout zebrafish line

To evaluate the effect of the long FLNA isoform on the development of the intestine, we used the zebrafish as an *in vivo* model. Reverse transcriptase-polymerase chain reaction (RT-PCR) results showed that *flna* is expressed in early embryonic stages starting at the four-cell stage, with increased expression throughout development (Fig. 4A). *In situ* hybridization also showed that *flna* is expressed in the brain and intestine of the zebrafish at all stages analyzed (Fig. 4B).

To generate the transgenic zebrafish line expressing only the short Flna isoform, we used two TALENs designed to target the region between the two methionine residues located in the first exon of *flna*. Considering that disruption of *NciI* restriction site would occur if the TALENs had successfully annealed, we used this enzyme to distinguish WT from transgenic fish (Supplementary Material, Fig. S1A). A deletion of six bps followed by

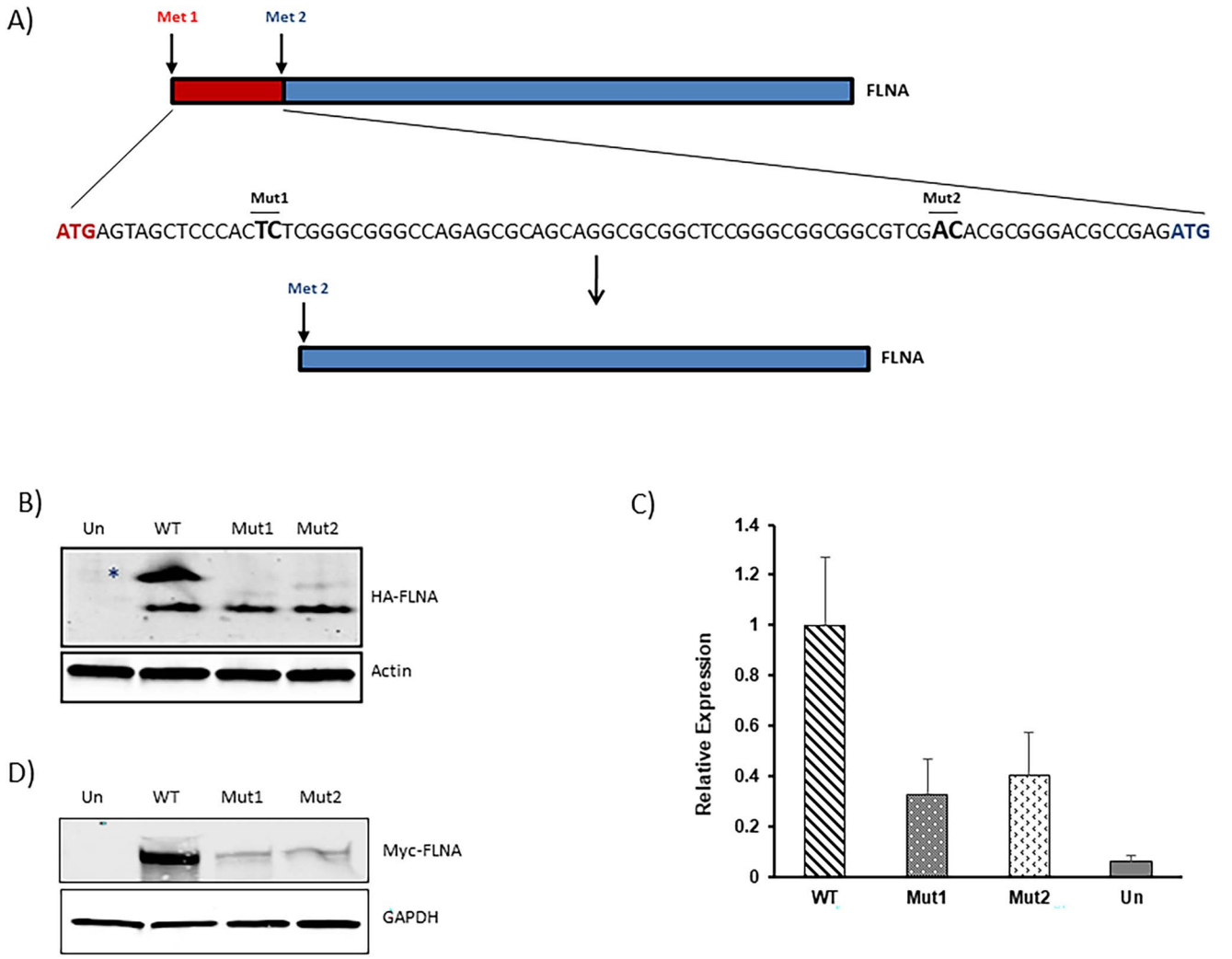

Figure 2. Absence of the long isoform results in decrease of FLNA expression. (**A**) Schematic representation of FLNA showing expression of two isoforms from a single transcript. In the presence of the 2-bp deletions identified in CIPO patients, only the short isoform is expressed (blue). (**B**) WB analysis of a mini gene construct expressing WT and mutant [Mut1(c.65-66delAC); Mut2 (c.16-17delTC)] versions of FLNA, show that two bands are expressed in the WT, while the mutants, express only one band. (**C**) qRT-PCR and (**D**) WB performed show reduced mRNA and protein levels in the mutants.

an insertion of one bp in a homozygous (*flna long isoform*$^{-/-}$) and in a heterozygous (*flna long isoform*$^{+/-}$) state, was identified in one male and one female fish, respectively (Supplementary Material, Fig. S1B). This in-frame deletion followed by an insertion, resulted in the appearance of an early stop codon at the end of exon 1, replicating the effect of the 2 bp deletions found in CIPO patients. Mutant fish were subsequently crossed to generate homozygous offspring lacking the long Flna isoform (*flna* long isoform$^{-/-}$). WB analysis showed that Flna protein was present in heterozygous and homozygous larvae (Supplementary Material, Fig. S1C), showing that the short Flna isoform was still expressed.

The long FLNA isoform is required for intestinal elongation

Since one of the features commonly seen in CIPO patients with *FLNA* mutations is the presence of CSBS, a dramatically shortened small intestine, we investigated the effect of disruption of the long FLNA isoform on the total length of the intestine of zebrafish larvae. Unlike humans, zebrafish do not have X and Y chromosomes, and carry two copies of the *flna* gene. Therefore, *flna long*$^{+/-}$ fish were analyzed together with homozygous mutant fish. The intestinal length of approximately 150 offspring (F3) was measured every day, for four days and revealed that the *flna long isoform*$^{-/-}$ zebrafish had a significantly shorter intestine compared with WT (0.318 mm ± 0.014 vs. 0.334 mm ± 0.015, respectively) (Fig. 5A). Disruption of only one of the *flna* alleles had no effect on the total length of the gut (0.331 mm ± 0.016 for *flna* long isoform$^{+/-}$ vs. 0.334 mm ± 0.015 for WT) (Fig. 5A). To exclude the possibility that the shortened intestine found in *flna long isoform*$^{-/-}$ fish was the result of an overall reduction in body length, the total length of each larva was also measured. However, the relative gut length–body length ratio remained significantly shorter in the *flna long isoform*$^{-/-}$ mutant fish (Fig. 5B).

Intestinal transit is reduced in the *flna long isoform* $^{-/-}$ transgenic zebrafish

Smooth muscle contractility is required for normal intestinal function. As our *in vitro* results showed that contractility of hiSMCs in the absence of the long FLNA isoform is affected, we decided to perform intestinal transit assays using our *flna* transgenic line. For these studies, 7-day old larvae (25 WT, 24 *flna* long isoform$^{+/-}$ and 35 *flna* long isoform$^{-/-}$) were fed for two hours with fluorescently labelled larval feed and imaged to

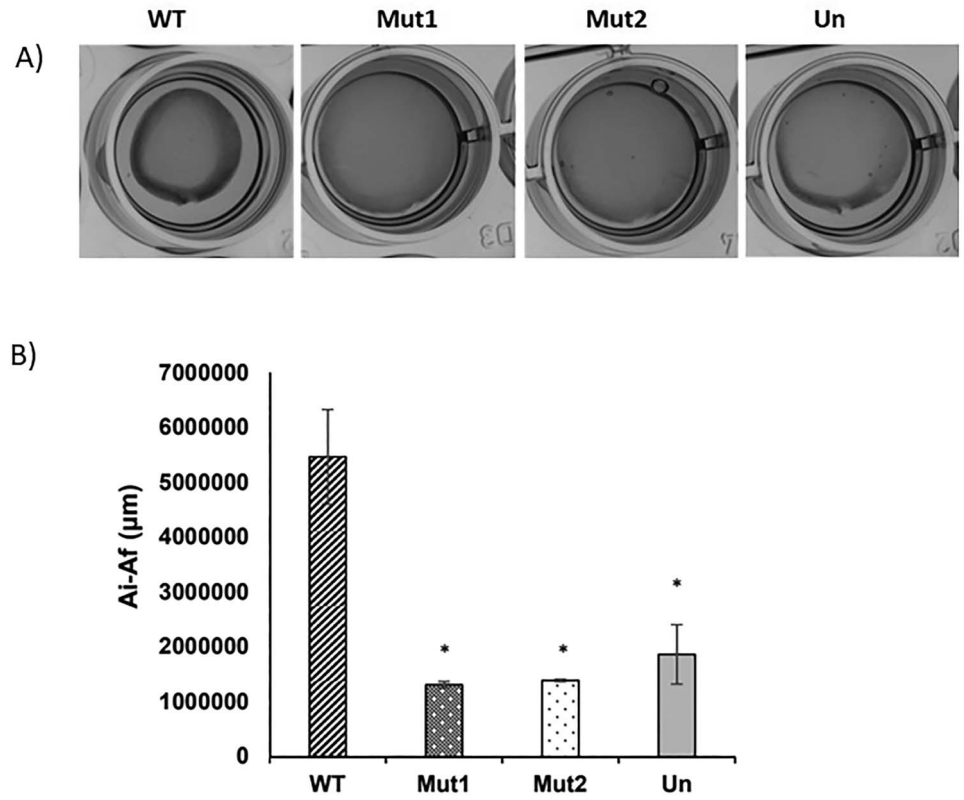

Figure 3. The long FLNA isoform is required for intestinal smooth muscle contractility, in vitro. (**A**) Contractility assays performed in human intestinal smooth muscle cells (hISMC) transfected with FLNA WT, Mut1 (c.16-17delTC) and Mut2 (c.65-66delAC), show an increase in contractility upon expression of FLNA WT, when compared with untrasnfected cells (Un). However this effect was lost in the presence of both mutants, Mut1 and Mut2. (**B**) Quantification of the difference between the initial (0 h) and final (24 h) area occupied by the collagen matrix, confirms altered contractility of hISMCs overexpressing Mut1 and Mut2. *$P < 0.05$. Ai: initial area; Af: final area.

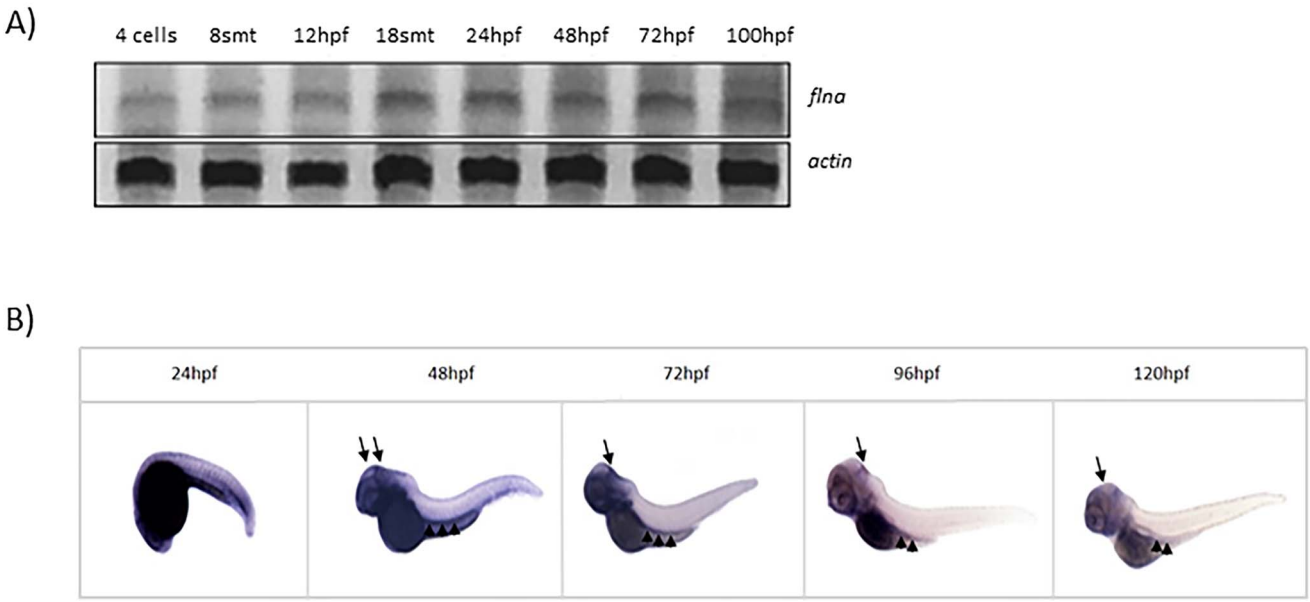

Figure 4. *flna* expression is detected in the zebrafish from early embryonic stages. (**A**) RT-qPCR performed in RNA isolated from zebrafish embryos at different embryonic stages shows that flna transcripts are present from as early as the 4-cell stage, and its expression increases during development. (**B**) *In situ* hybridization shows that flna is highly expressed in the brain (arrows) and gut (arrowheads) of the zebrafish at different stages of development. Smt—somites; hpf—hours post fertilization.

select the ones that showed fluorescence in their intestinal bulb (Fig. 5C). Twenty-four hours later, these larvae were imaged again, and we observed that while the majority of WT and heterozygous fish no longer showed fluorescence within the GI tract (76% and 83% respectively), only 57% of homozygous fish showed the same (Fig. 5C and D).

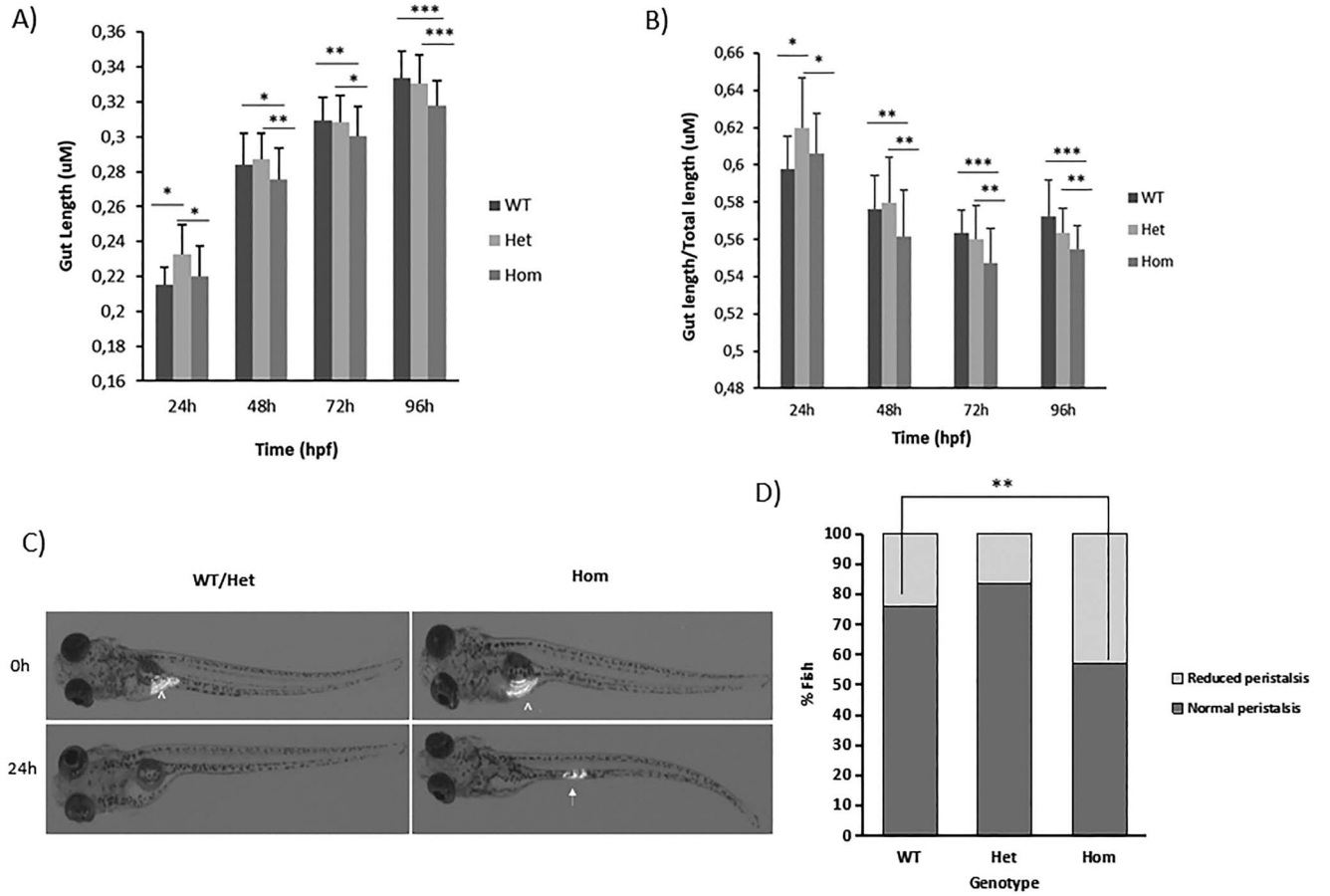

Figure 5. *flna long*$^{-/-}$ zebrafish have shorter small intestines and increased transit time. (**A**) Measurement of the intestinal length of WT and transgenic fish shows that *flna long isoform*$^{-/-}$ (hom) embryos have significantly shorter intestines, when compared with WT and *flna long isoform*$^{+/-}$ (het). (**B**) No effect of the body length was detected. (**C**) WT, *flna long isoform*$^{+/-}$ and *flna long isoform*$^{-/-}$ larvae were screened for the presence of fluorescence microspheres in the intestinal bulb (arrowheads). (**D**) *flna long isoform* $^{-/-}$ (hom) larvae have longer transit time (43%) compared with WT (24%) and *flna long isoform*$^{+/-}$ (17%; het) fish. Hpf—hours post-fertilization; *$P < 0.05$; **$P < 0.005$; ***$P < 0.00005$.

To exclude the possibility that the motility defect observed in the *flna* long isoform$^{-/-}$ was a result of reduced numbers of enteric neurons present in the Enteric Nervous System (ENS), we decided to quantify these cells in the gut of WT, heterozygous and homozygous 5 dpf larvae ($n = 16$, 46 and 11, respectively). We found no significant differences (31.043 neurons ±3.226 vs. 30.504 neurons ±3.757 vs. 31.552 neurons ±2.384, respectively) between the groups (Fig. 6A and B). Additional immunohistochemistry studies using the pan-neuronal marker HuC/D, revealed normal distribution of enteric neurons in between the inner and outer smooth muscle layers (sml) for the *flna* long isoform$^{-/-}$ fish (Fig. 6C, green arrow).

Diffuse abnormal layering of the intestinal smooth muscle is observed in *flna* long isoform $^{-/-}$ adult fish

Previous studies have shown that CIPO patients in which the long FLNA isoform is missing, presented a diffused abnormal layering of small intestinal smooth muscle (13). To investigate if similar changes were present in our *flna* long isoform$^{-/-}$ adult fish, hematoxylin staining was performed in full-thickness sections. Our results showed that the muscularis propria of WT and mutant zebrafish was composed by two distinct layers: outer layer or longitudinal smooth muscle (lsm), and inner layer or circular smooth muscle (csm). This is in agreement with previous reports (13). However, in the *flna* long isoform$^{-/-}$ fish, we interestingly found hypertrophy of the lsm (Fig. 7A). Additional staining for α-smooth muscle actin (ACTA2), confirmed a thicker and diffuse abnormal layering of the muscularis propia of homozygous fish and showed the presence of a prominent muscularis mucosae layer that is not visible in the WT or heterozygous fish (Fig. 7B, blue arrow). These results show that structural and architectural changes are present in the intestinal smooth muscle of the *flna* long isoform$^{-/-}$ adult fish.

Expression of smooth muscle markers are affected in *flna* long isoform$^{-/-}$ fish

To further investigate the reasoning behind the histological changes detected in the homozygous fish, we determined the expression levels of intestinal smooth muscle markers, *acta2*, *sm22α-b* and *calponin1*, by qRT-PCR (14). The first two, are early developmental markers, whereas calponin 1 is specific for differentiated smooth muscle. We decided to look at the expression of these markers at two time points, at 7dp when the larvae start eating and the intestine is functional, and in the adult stage. The levels of *flna* present in larvae and adult fish, were also determined for the three genotypes. Our results showed that changes in the expression of smooth muscle markers are indeed present in the *flna long isoform*$^{-/-}$ fish. *acta2* was significantly downregulated in homozygous larvae, when compared with

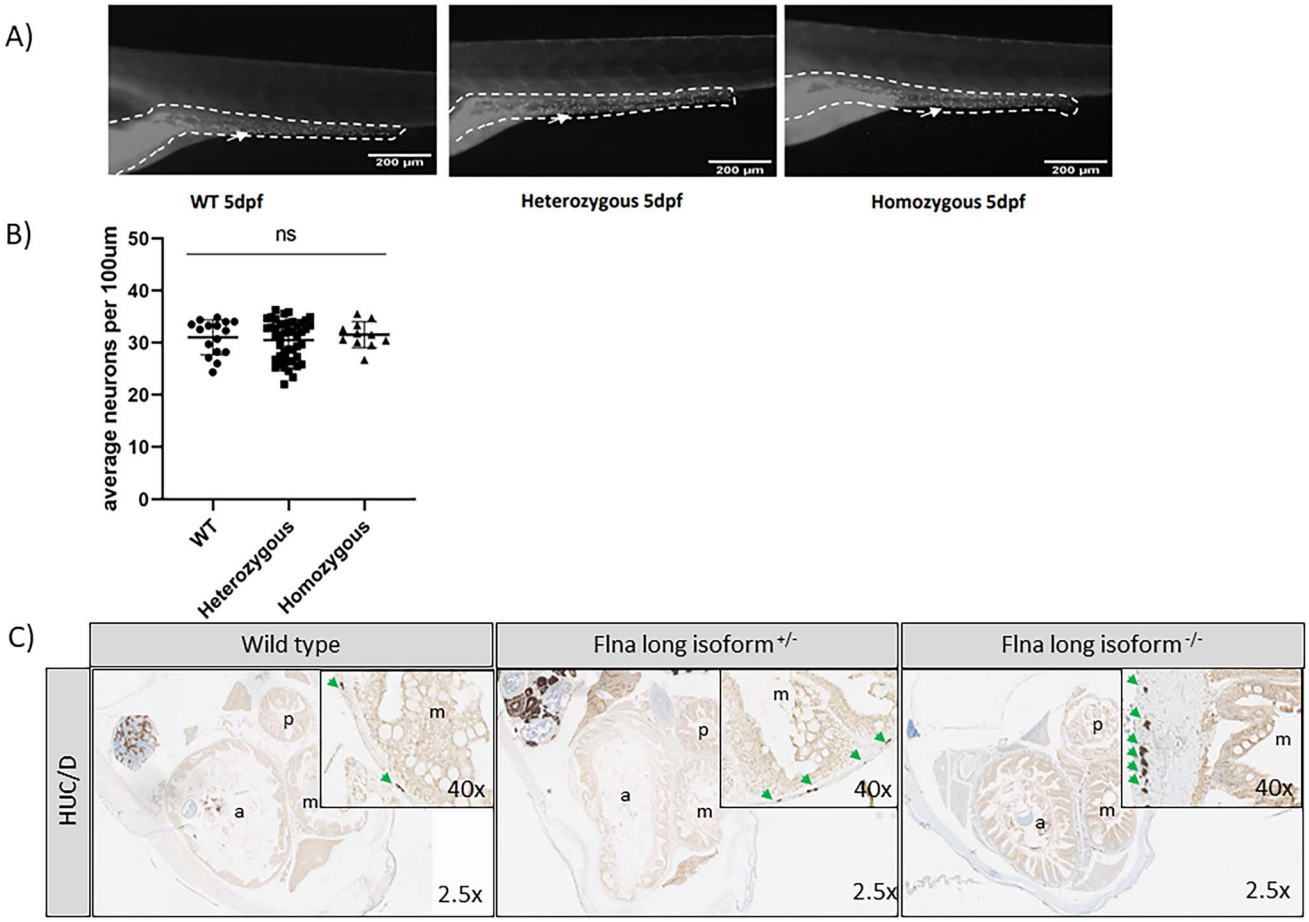

Figure 6. Enteric neuronal numbers and localization are not affected in *flna long isoform*$^{-/-}$ larvae. (**A**) Whole mount staining of WT, *flna long isoform*$^{+/-}$ (heterozygous) and *flna long isoform*$^{-/-}$ (homozygous) 5dpf fish, was performed with an HuC/D antibody, to label enteric neurons (pointed by white arrow). (**B**) Quantification of the number of enteric neurons present in WT, heterozygous and homozygous larvae showed no difference on the neuronal density of the gut between genotypes. Ns = not significant. (**C**) HuC/D stainings performed in adult fish showed a similar distribution and localization of enteric neurons for WT, heterozygous and homozygous fish (green arrow).

heterozygous and control fish. However, in adult stages, an increase in the expression level of acta2 was significantly detected. For *sm22α-b*, a decrease expression was observed in homozygous larvae and adult fish when compared with WT fish, while *calponin1*, was increased (Fig. 7C). Interestingly, the levels of *flna* were significantly upregulated in both heterozygous and homozygous larvae, and this pattern was maintained in adulthood but only in the *flna* long isoform$^{-/-}$ fish (Fig. 7C). This is likely to be a compensatory mechanism.

Discussion

FLNA has been extensively studied as pathogenic variants in its coding region have been associated with a broad spectrum of disorders collectedly referred to as X-linked filaminopathies (4). To date, loss and gain of function variants in *FLNA* are associated with eight syndromes, including CIPO, a heterogeneous gastrointestinal disorder characterized by compromised intestinal motility (8,11,12). Interestingly, these variants are two bp deletions located in between two different transcription starting sites, and they have recently been shown to block expression of the long FLNA isoform (12). In addition, the long FLNA isoform was observed to be the predominant one in ileum and colon, as well as in colonic smooth muscle (12). Based on our results, abundant expression of FLNA was indeed detected in the small intestine during human embryonic development, specifically in the smooth muscle cells (SMCs) of the muscularis mucosa and muscularis propria (Fig. 1). However, we were unable to distinguish expression of the different FLNA isoforms, due to the absence of specific commercially available antibodies. Our mini-gene assays confirmed the presence of two initiation codons in FLNA and showed that CIPO causing *FLNA* variants, lead to the adoption of the second initiation codon, resulting in the expression of only the short isoform (Fig. 2B). Considering that the long isoform has been shown to be the major FLNA isoform expressed in intestinal smooth muscle (12), it is not surprising that these patients only have intestinal complaints, with the majority of them being diagnosed with CIPO. Taken these results together, it is tempting to say that loss of the long FLNA isoform in CIPO patients, affects intestinal SMCs. Such concept has already been suggested before based on the analysis of the neuromuscular histopathology of CIPO patients with *FLNA* variants (13). Therefore, our results are in line with previous findings, confirming a myopathic nature for CIPO in these cases.

Previous studies have shown that disruption of the first 32 amino acids of FLNA, does not impact FLNA co-localization with actin, neither its actin-binding ability (15). However, selective disruption of *Flna* in the smooth muscle of adult mice, showed that Flna is involved in signalling cascades for smooth muscle contractility (16). In line with this study, we observed that expres-

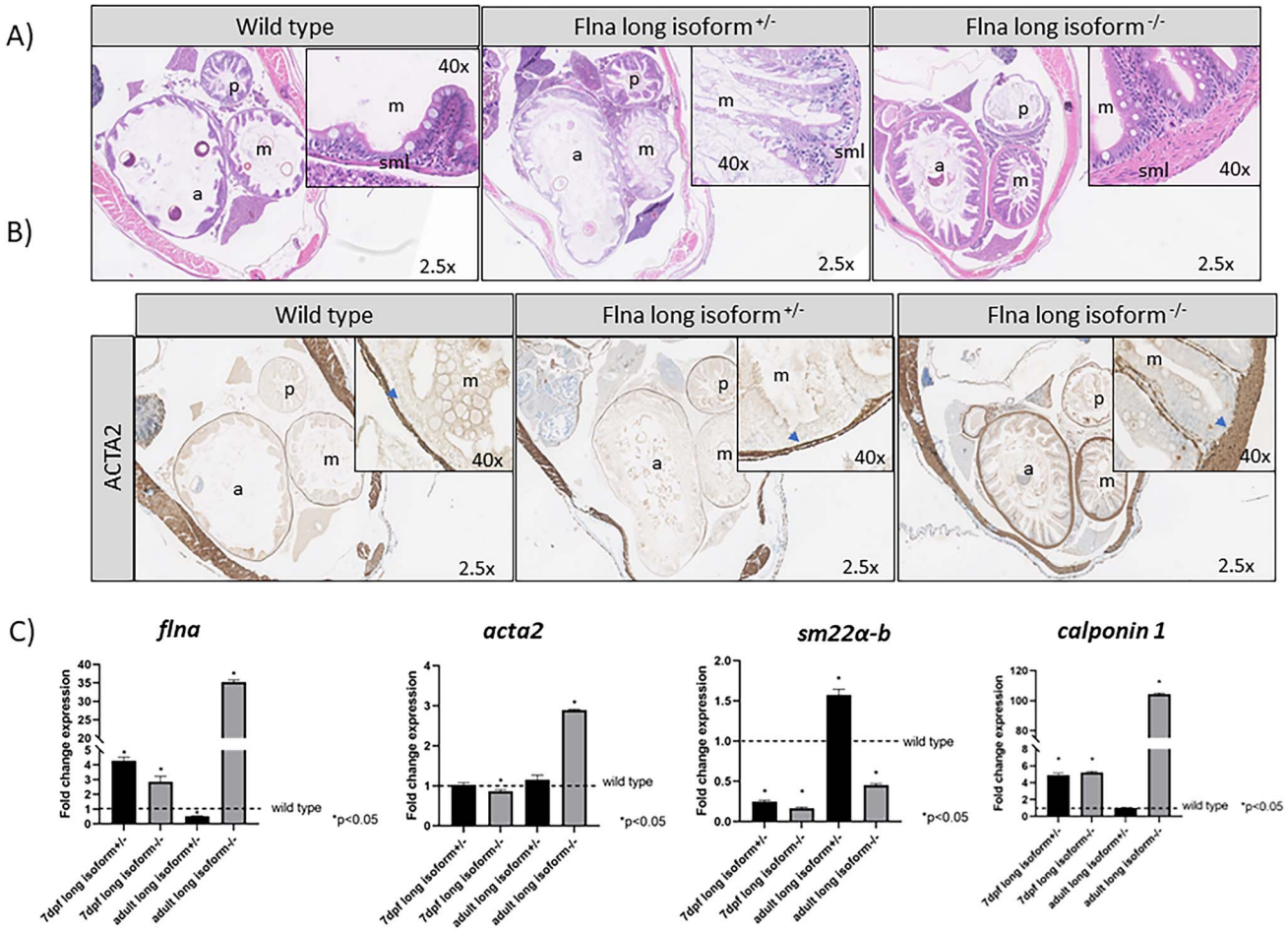

Figure 7. *flna long isoform*$^{-/-}$ zebrafish show hypertrophy and abnormal layering of the intestinal smooth muscle, as well as altered expression of smooth muscle markers. (**A**) Hematoxylin staining showed the presence of a thick and diffuse abnormal layering in muscularis propria of homozygous adult fish. Low to high magnification images are presented. (**B**) Acta2 staining confirmed hypertrophy of the intestinal smooth muscle in *flna long isoform*$^{-/-}$ adult fish, and revealed an extra muscularis mucosae layer (blue arrow) that is not present in the WT or heterozygous fish. Low to high magnification images are presented. (**C**) qRT-PCR revealed altered expression (*$p < 0.05$) of intestinal smooth muscle markers in 7dpf homozygous larvae and adult zebrafish. sml: smooth muscle layer; a: anterior gut; p: posterior gut; m: mid-gut.

sion of only the short isoform, leads to expression changes that impact cellular contractility (Fig. 3A and B), suggesting that FLNA levels are instrumental for intestinal smooth muscle contraction To further investigate these findings, we generated a transgenic zebrafish line in which expression of the long *flna* isoform was abolished. We observed that *flna long isoform*$^{-/-}$ larvae had significantly shortened intestines (Fig. 5A), suggesting that the long FLNA isoform is important for intestinal elongation. This data also explains why the majority of CIPO patients carrying *FLNA* mutations are born with CSBS. To our surprise, the reduction observed in intestinal length was limited to 5%, which is far below the reduction observed in CSBS patients (>75%). This discrepancy can be attributed to anatomical differences, as the fish gut is just a simple linear tube with no defined regions, while in humans it is very elongated and requires complex patterns of rotation and looping to reach its final configuration. We also cannot exclude the involvement of other proteins with a redundant function in the zebrafish. Previous studies have shown that three other genes are known to encode for *flna* homologs in the fish, which include *flnb*, *flnca* and *flncb* (17,18). Although the function of all flna proteins is not yet clear, shared characteristics between all homologs suggest possible functional redundancy. Our *flna long isoform*$^{-/-}$ larvae also showed increased intestinal transit time, when compared with WT and *flna long isoform*$^{+/-}$ fish (Fig. 5C and D), suggesting that intestinal motility is affected by the loss of the long FLNA isoform. Histological examination of the intestine of adult homozygous fish revealed hypertrophy of the smooth layer and showed the presence of what seems to be an extra muscularis mucosae layer (Fig. 7A and B). Similar findings have been described for CIPO patients carrying *FLNA* variants (13). Moreover, we observed altered expression of intestinal smooth muscle markers in *flna long isoform*$^{-/-}$ larvae and adult fish, that can potentially underlie the structural changes identified (Fig. 7C). Since we found no differences in the distribution and number of enteric neurons present in WT, *flna long isoform*$^{+/-}$ and *flna long isoform*$^{-/-}$ (Fig. 6), it seems that the GI defects observed in CIPO patients with *FLNA* deletions, are likely due to a defect in smooth muscle contractility caused by the absence of the long FLNA isoform. However, we cannot exclude that possible defects in the anatomy or physiology of the ENS might still exist.

In summary, our data confirm the presence of two FLNA isoforms and show that the long isoform plays an instrumental role in intestinal elongation and smooth muscle contractility, bringing new insights to CIPO pathogenesis. We also confirm that

the zebrafish is an excellent animal model to study intestinal development, specifically congenital intestinal myopathies, as the phenotype of our homozygous fish showed great similarities to the one previously described for CIPO patients (13).

Materials and Methods

Immunohistochemistry in human small intestinal specimens

Paraffin-embedded human small intestinal specimens from controls were collected at weeks 17 and 22 of embryonic development, at neonatal stage and at a post-natal stage at 3 months of age, from the department of Pathology, Erasmus University Medical Center. Slides were stained with a specific antibody against FLNA (dilution 1:1000; Eurogentec, Seraing, Belgium), using a previously described protocol (19).

Expression vectors and site-directed mutagenesis

pAAV2.1-CMV-EGFP-FLNA wild-type (WT) and pAAV2.1-CMV-EGFP-FLNA mutant 2 (Mut2, c.65-66delAC) constructs were kindly provided by Prof. Alberto Auricchio from the University of Napoli. pCMV6-FLNA(Myc-DDK) was purchased from OriGene (Rockeville, Maryland, USA).

pAAV2.1-CMV-EGFP-FLNA mutant 1 (Mut1, C.16-17delTC), pCMV6-FLNA(Myc-DDK)mut1 (c.16-17delTC) and pCMV6-FLNA-(Myc-DDK)mut 2 (c.65-66delAC) were generated by site-directed mutagenesis according to the Q5 Site Directed Mutagenesis manufacturer's instructions (New England Biolabs, Ipswich, Massachusetts, USA), using the WT constructs. Primers used for site directed mutagenesis are described in Supplementary Material, Table S1.

Cell culture and transfection

Human embryonic kidney cells (HEK293) were cultured in DMEM with high glucose content supplemented with 10% FBS and 1% penicillin/streptomycin. Human intestinal smooth muscle cells (hiSMCs) were obtained from ScienceCell (Carlsbad, California, USA) and cultured according to the instructions provided. All cells were incubated at 37°C in the presence of 5% CO_2.

For transient transfection, 300 000 cells of HEK293 and 500 000 of hiSMCs were cultured in a 6 well plate. Twenty-four hours after, cells were transfected with 1 μg of plasmid DNA using GeneJuice (Millipore, Burlington, Massachusetts, USA) as transfection reagent, according to the manufacturer's instructions.

Cell lysis and western blot

Cells were lysed 48 hours after transfection using m-PER (Thermo Scientific, Waltham, Massachusetts, USA) and 1X protease inhibitors (Roche, Basel, Switzerland). Cell lysate preparation, protein quantification and WB analysis were performed as described before (19). The following antibodies were used: anti-HA (Cell Signaling Technology, Danvers, Massachusetts, USA), anti-Myc (Cell Signaling Technology, Danvers, Massachusetts, USA), anti-FLNA (Abcam, Cambridge, UK), anti-GAPDH (Millipore, Burlington, Massachusetts, USA) and anti-actin (Santa Cruz Biotechnologies, Dallas, Texas, USA). Secondary antibodies used were IRDye 800CW Goat anti-mouse, IRDye 680RD Goat anti-Rabbit and IRDye 680RD Donkey anti-Goat (Li-Cor, Lincoln, Nebraska, USA).

RNA isolation, cDNA preparation, RT-PCR and qRT-PCR

Zebrafish larvae collected at different embryonic stages were lysed in Trizol. RNA isolation from zebrafish larvae and cell lines was performed with the RNeasy mini kit (Qiagen, Hilden, Germany), according to the manufacturer's instructions. 1 μg of RNA was used for cDNA preparation with the iScript cDNA Synthesis Kit (Bio-Rad, Hercules, California, USA). For RT-PCR, 100 ng/μl of cDNA was used as template. For qRT-PCR, relative expression was quantified using the $2^{-\Delta\Delta Ct}$ method and normalized to actin and GAPDH. Primers used can be found in Supplementary Material, Table S1.

Cell contractility assays

Twenty-four hours after transfection, 2 X 10^6 hiSMCs expressingp-CMV6-FLNA(Myc-DDK)WT, pCMV6-FLNA(Myc-DDK)Mut1 and pCMV6-FLNA(Myc-DDK)Mut2 were trypsinized, mixed with collagen (Cell Biolabs, San Diego, California, USA) and platted in 24 well plates (19). One day later, collagen matrixes were dislodged from the wells and cellular contractility was measured 12–18 h after. Untransfected cells (un) were used as controls.

Animals

The Tupfel long (TL) fin zebrafish strain was used for all *in vivo* experiments described in this manuscript. Adult and larval fish were maintained on a 14 h/10 h light–dark cycle at 28°C. Animal experiments were approved by the Animal Experimentation Committee of the Erasmus Medical Center.

Whole mount *in situ* hybridization

RNA isolated from 48 h post fertilization (hpf) larvae was used as a template for cDNA using a One-Step RT-PCR kit (Qiagen, Hilden, Germany). Primers used for amplification are described in Supplementary Material, Table S1. Amplified bands were subcloned into the TOPO TA PCRII cloning vector (Thermo Fisher Scientific, Waltham, Massachusetts, USA). Digoxigenin labelled anti-sense probes (Roche, Basel, Switzerland) were generated by linearizing the plasmids with *NotI* (New England Biolabs, Ipswich, Massachusetts, USA), then transcribed with SP6 polymerase (Roche, Basel, Switzerland). *In situ* hybridization was performed on staged zebrafish larvae as previously described (20).

Generation of the *flna* long isoform knockout zebrafish

TALENs were designed to target exon one of *flna* and recognize the following sequences: 5′- CCCCTATCCAACGCTTC and 3′- GACGC-CGACATGCCCGC. To establish the *flna* long knockout mutant fish, 100 pg mRNA of each TALEN was injected into the cell of a one-cell stage embryo collected from WT zebrafish crossings. All injected embryos were raised to adulthood and crossed to generate F1. F1 transgenic larvae were raised to adulthood and genotyped. One homozygous fish containing a 6 base-pair deletion followed by a 1 base-pair insertion was crossed with a heterozygous fish containing the same genetic alteration. F2 transgenic fish were generated, raised to adulthood, and genotyped. All *in vivo* experiments described in this manuscript were performed in F3 fish.

Genotyping of transgenic zebrafish

Finclips of transgenic zebrafish were used for DNA isolation using a mixture containing Tris–HCl (pH 9.0), KCl, Triton X-100 and protease K (Sigma Aldrich, St. Louis, Missouri, USA). After incubation at 55°C for one hour, protease K was inactivated at 98°C for

10 min. Isolated DNA was used as a template for a PCR reaction with a standard program. Primers are described in Supplementary Material, Table S1. The PCR product was subjected to restriction digestion with *NciI* (New England Biolabs, Ipswich, Massachusetts, USA) for 1 h at 37°C. In parallel, the PCR product was submitted to Sanger sequencing, which was performed with dye labelled primers (Big Dye Terminator v3.1 Sequencing Kit, Applied Biosystems, Waltham, Massachusetts, USA) on ABI 3130XL genetic analyzer. Sanger reads were analyzed using SeqScape software.

Intestinal length measurements in zebrafish

Zebrafish larvae were collected after fertilization and individually placed in a 24-well plate. Each larva was imaged every 24 h under the microscope (Leica DFC550, Leica Camera, Wetzlar, Germany) for 4 days. Gut measurements were made using Fiji Image J software and based on the distance from mouth and vent. All larvae were genotyped at the end of the experiment. Statistical significance was calculated using a two-paired *t*-test.

Intestinal transit assays in zebrafish

Seven-days old zebrafish larvae were fed for two hours with a mixture containing 100 mg of powdered larval feed, 150 μl of fluorescent 2.0 μm polystyrene microspheres (Invitrogen) and 50 μl of water. After 2 h, larvae were anesthetized with Tricaine and were checked under the microscope (Leica DFC550, Leica Camera, Wetzlar, Germany) for the presence of fluorescent food in their intestine. Individual larvae were placed in separate wells of a 24-well plate and examined 24 h after feeding under the microscope. All larvae were genotyped at the end of the experiment.

Enteric neuronal density analysis in zebrafish

Zebrafish larvae at 5 days post fertilization (dpf), previously treated with phenyl thiourea at 1dpf to prevent the pigmentation, were used for enteric neuronal density analysis. Larvae were incubated on ice for 30 min before being fixed in 4% paraformaldehyde (PFA) and washed in 1x phosphate buffer solution/0.25% Triton X-100 for 1 h, at room temperature. Whole mount antibody staining was performed according to previous reports (21). Anti HuC/HuD (1:1000, Invitrogen, Waltham, Massachusetts, USA) was used as primary antibody and the Alexa Fluor 488 Mouse IgG (1:2000, Thermo Fisher Scientific, Waltham, Massachusetts, USA) as secondary antibody. Larvae were observed under the fluorescent microscope (Leica M165FC, Leica Camera, Wetzlar, Germany) using the GFP filter. Images of the intestine were taken, and the number of enteric neurons were counted using Fiji Image J software. All larvae were genotyped at the end of the experiment. Statistical significance was calculated using an one-way analysis of variance test.

Immunohistochemistry

Adult zebrafish were sacrificed and fixated in 4% PFA overnight. Fish were fixed in 1.8% low-melting-point agarose and proceeded with paraffin embedding. Ten μm sections were cut with the microtome and immunohistochemical staining was performed using the Ventana Benchmark Ultra automated staining system (Ventana Medical System, Tuscon, AZ, USA). Briefly, antigen retrieval was performed on sectioned specimens for 60 min after deparaffinization, using the Cell Conditioning Solution (CC1, Ventana 950-124). After 30 min, incubation with the primary antibody was performed at 36°C (ACTA2 1:2000; GTX124505; Genetex and HuC/D, 1:50; A-21271, Molecular Probes), followed by amplification with the Ultraview amplification kit (Ventana 760-080), and detection with the UltraView Universal DAB detection kit (Ventana 760-500). Sections were counterstained with hematoxylin II (Ventana 790-2208). Images were taken using Olympus DP72 digital camera microscope and analyzed with Olympus cellSense software (Olympus, Tokyo, Japan).

Supplementary Material

Supplementary Material is available at *HMG* online.

Acknowledgements

The authors would like to thank Prof. Alberto Auricchio for kindly providing the pAAV2.1-CMV-EGFP-FLNA WT and pAAV2.1-CMV-EGFP-FLNA mutant 2 (Mut2, c.65-66delAC) constructs, and Dr Marion Gijbels from the University of Maastricht, for valuable insights in the interpretation of the histological data obtained for the zebrafish.

Conflict of Interest statement. No conflicts of interest exist.

Funding

This work was supported by a grant from the Sophia foundation awarded to MMA and RMWH (SSWO 17-18).

References

1. Onoprishvili, I., Ali, S., Andria, M.L., Shpigel, A. and Simon, E.J. (2008) Filamin A mutant lacking actin-binding domain restores mu opioid receptor regulation in melanoma cells. *Neurochem. Res.*, **33**, 2054–2061.
2. Nakamura, F., Stossel, T.P. and Hartwig, J.H. (2011) The filamins: organizers of cell structure and function. *Cell Adhes. Migr.*, **5**, 160–169.
3. Robertson, S.P. (2005) Filamin A: phenotypic diversity. *Curr. Opin. Genet. Dev.*, **15**, 301–307.
4. Wade, E.M., Halliday, B.J., Jenkins, Z.A., O'Neill, A.C. and Robertson, S.P. (2020) The X-linked filaminopathies: synergistic insights from clinical and molecular analysis. *Hum. Mutat.*, **41**, 865–883.
5. Kyndt, F., Gueffet, J.P., Probst, V., Jaafar, P., Legendre, A., Le Bouffant, F., Toquet, C., Roy, E., McGregor, L., Lynch, S.A. *et al.* (2007) Mutations in the gene encoding filamin A as a cause for familial cardiac valvular dystrophy. *Circulation*, **115**, 40–49.
6. Bernstein, J.A., Bernstein, D., Hehr, U. and Hudgins, L. (2011) Familial cardiac valvulopathy due to filamin A mutation. *Am. J. Med. Genet. Part A*, **155**, 2236–2241.
7. Oegema, R., Hulst, J.M., Theuns-Valks, S.D.M., van Unen, L.M.A., Schot, R., Mancini, G.M.S., Schipper, M.E.I., de Wit, M.C.Y., Sibbles, B.J., de Coo, I.F.M. *et al.* (2013) Novel no-stop FLNA mutation causes multi-organ involvement in males. *Am. J. Med. Genet. Part A*, **161**, 2376–2384.
8. Van Der Werf, C.S., Sribudiani, Y., Verheij, J.B.G.M., Caroll, M., O'Loughlin, E., Chen, C.H., Brooks, A.S., Liszweski, M.K., Atkinson, J.P. and Hofstra, R.M.W. (2013) Congenital short bowel syndrome as the presenting symptom in male patients with FLNA mutations. *Genet. Med.*, **15**, 310–313.
9. Gamboa, H.E. and Sood, M. (2019) Pediatric intestinal pseudo-obstruction in the era of genetic sequencing. *Curr. Gastroenterol. Rep.*, **21**, 70.
10. Thapar, N., Saliakellis, E., Benninga, M.A., Borelli, O., Curry, J., Faura, C., De Giorgia, R., Gupte, G., Knowles, C.H., Staiano, A. *et al.* (2018) Paediatric intestinal pseudo-obstruction: evidence

and consensus-based recommendations from an ESPGHAN-led expert group. *J. Pediatr. Gastroenterol. Nutr.*, **66**, 991–1019.
11. Gargiulo, A., Auricchio, R., Barone, M.V., Cotugno, G., Reardon, W., Milla, P.J., Ballabio, A., Ciccodicola, A. and Auricchio, A. (2007) Filamin A is mutated in X-linked chronic idiopathic intestinal pseudo-obstruction with central nervous system involvement. *Am. J. Hum. Genet.*, **80**, 751–758.
12. Jenkins, Z.A., Macharg, A., Chang, C.Y., van Kogelenberg, M., Morgan, T., Frentz, S., Wei, W., Pilch, J., Hannibal, M., Foulds, N. *et al.* (2018) Differential regulation of two FLNA transcripts explains some of the phenotypic heterogeneity in the loss-of-function filaminopathies. *Hum. Mutat.*, **39**, 103–113.
13. Kapur, R.P., Robertson, S.P., Hannibal, M.C., Finn, L.S., Morgan, T., van Kogelenberg, M. and Loren, D.J. (2010) Diffuse abnormal layering of small intestinal smooth muscle is present in patients with FLNA mutations and X-linked intestinal pseudo-obstruction. *Am. J. Surg. Pathol.*, **34**, 1528–1543.
14. Georgijevic, S., Subramanian, Y., Rollins, E.L., Starovic-Subota, O., Tang, A.C.Y. and Childs, S.J. (2007) Spatiotemporal expression of smooth muscle markers in developing zebrafish gut. *Dev. Dyn.*, **236**, 1623–1632.
15. Iwamoto, D.V., Huehn, A., Simon, B., Huet-Calderwood, C., Baldassarre, M., Sindelar, C.V. and Calderwood, D.A. (2018) Structural basis of the filamin a actin-binding domain interaction with F-actin. *Nat. Struct. Mol. Biol.*, **25**, 918–927.
16. Retailleau, K., Arhatte, M., Demolombe, S., Peyronnet, R., Baudrie, V., Jodar, M., Bourreau, J., Henrion, D., Offermans, S., Nakamura, F. *et al.* (2016) Arterial myogenic activation through smooth muscle filamin a. *Cell Rep.*, **14**, 2050–2058.
17. Bandaru, S., Zhou, A.X., Rouhi, P., Zhang, Y., Bergo, M.O. and Akyurek, L.M. (2014) Targeting filamin B induces tumor growth and metastasis via enhanced activity of matrix metalloproteinase-9 and secretion of VEGF-A. *Oncogene*, **3**, e119.
18. Ruparelia, A.A., Zhao, M., Currie, P.D. and Bryson-Richardson, R.J. (2012) Characterization and investigation of zebrafish models of filamin-related myofibrillar myopathy. *Hum. Mol. Genet.*, **21**, 4073–4083.
19. Halim, D., Hofstra, R.M.W., Signorile, L., Verdijk, R.M., van der Werf, C.S., Sribudiani, Y., Brouwer, R.W.W., van IJcken, W.F.J., Dahl, N., Verheil, J.B.G.M. *et al.* (2016) ACTG2 variants impair actin polymerization in sporadic megacystis microcolon intestinal hypoperistalsis syndrome. *Hum. Mol. Genet.*, **25**, 571–583.
20. Thisse, B. and Thisse, C. (2014) In Situ Hybridization on Whole-Mount Zebrafish Embryos and Young Larvae. *Methods Mol Biol.*, **1211**, 53–67.
21. Uyttebroek, L., Shepherd, I.T., Harrisson, F., Hubens, G., Blust, R., Timmermans, J.P. and van Nassauw, L. (2010) Neurochemical coding of enteric neurons in adult and embryonic zebrafish (*Danio rerio*). *J. Comp. Neurol.*, **518**, 4419–4438.